A large, stylized pink awareness ribbon is centered on the page. The ribbon is a vibrant shade of pink with a slight gradient and a soft shadow, giving it a three-dimensional appearance. It is positioned behind the title and author information.

Laser Irradiation of Tumors for the Treatment of Cancer: An Analysis of Blood Flow, Temperature and Oxygen Transport

BEE 453

May 4, 2007

Ravi Sood, David Nahlik, Weston Nichols, and Evan Graham

Executive Summary

It has been shown that hypoxic tumor cells are resistant to radiation and that increasing tumor oxygen levels via laser-mediated hyperthermia treatment increases tumor cell radiosensitivity. Hence, studies of the effects of laser irradiation on tumor oxygen levels are of great interest, as they allow for the optimization of hyperthermia treatment. Accordingly, the main purpose of this experiment was to develop a finite element model to simulate the heat transfer due to laser irradiation of tumor tissue, the blood flow through a tumor capillary, and the effect of changing temperature on blood flow rates and oxygen delivery to tumor tissue. This was achieved by using finite element models in COMSOL Multiphysics. We employed two geometries based on those used in a similar study by He et al. [1]: a tumor-containing breast model to simulate laser heating of the tissue and a capillary and tumor tissue model to simulate the effect of heating on blood flow and tissue oxygen concentration. By plotting partial pressure of oxygen as a function of radius at three different points in the tissue, we observed that the oxygen concentration was greatest near the inlet and lowest near the outlet (as expected), and that at all points in the tissue, heating increased the tissue oxygen partial pressure to about the same extent (0.75 – 1 mm Hg). Furthermore, sensitivity analyses suggested ambient air cooling at the breast surface to be ideal and a laser intensity of 18000 W/m^2 to be optimal for hyperthermia treatment. The model we developed was validated by comparison to a similar model and has potential for use in future studies on optimization of hyperthermia treatment.

Introduction

According to the American Cancer Society, approximately 15% of the 678,060 cases of cancer estimated for women in 2007 will be some form of breast cancer [2]. This means that approximately 101,709 women will be afflicted this year. Breast cancer is the second most common form of cancer for women, preceded only by lung and bronchus cancers which are estimated to afflict approximately 29% of female cancer patients this year [2]. The incidence rate of breast cancer among women, however, has begun to level off after a sharp increase in the 1980s due to the increased use of X-ray mammography.

Breast cancer can begin in any of the various tissues of the breast, including milk producing lobules, duct tubules through which this milk is transported, blood and lymph vessels, fatty tissue, and connective tissues. Below is a schematic taken from the American Cancer Society which illustrates the situation of these cellular systems within the female breast.

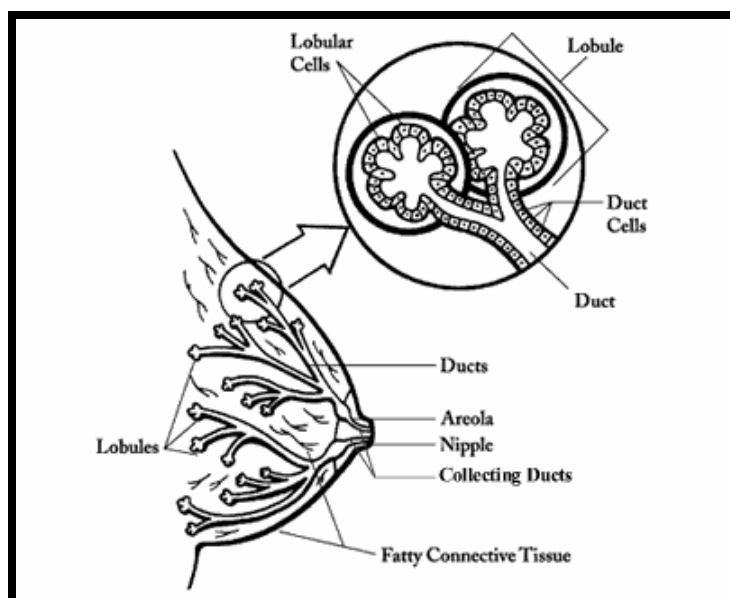


Figure 1 Pictorial representation of the tissues and cellular systems found in the female.

While highly uncommon, breast cancer can occur in males, but because of the considerable amount of breast cells that most women possess compared to most men, cancer is understandably more prevalent in the female population.

One of the oldest and most successful treatments of breast cancer to date is invasive surgery; however, alternative, slightly less invasive methods of treatment are being explored, one of which is radiation therapy. Laser irradiation works best for cancers that are rapidly or actively dividing, and recent research suggests that it enhances radiosensitivity of dividing cells by enhancing oxygenation of the tumor tissues [2]. This oxygenation is thought to be caused by increased blood perfusion coupled with a decreased oxygen consumption rate due to mild hyperthermia [3]. Another study of the effect of irradiation on tumor cells showed that the process of radiosensitization is linked to G₂/M arrest and apoptosis of cancerous (or normal) cells [4]. However, further investigation on the use of hyperthermia in conjunction with radiotherapy is necessary to study the effects of this technique on normal tissues as well as to quantify the

oxygen concentration gradients created by the dilation and increased permeability of breast blood vessels due to the increase in temperature.

Accordingly, the focus of this project was the development of a mathematical model to simulate the heat transfer due to laser irradiation of tumor cells, the blood flow through a tumor capillary, and resulting changes in flow rates and oxygen delivery to tumor tissue. We adopted the following schematics from He et al. [1] to model the effect of temperature (modeled in the breast geometry) on blood flow and oxygen diffusion in a capillary in the tumor (modeled in the blood vessel geometry). These simplifications allowed us to develop a model to analyze the effects of temperature on blood flow rate and oxygen concentration in the tumor that could be used to optimize parameters of hyperthermia treatment. As a preliminary step, we studied the effects of varying laser intensity and cooling conditions at the breast surface.

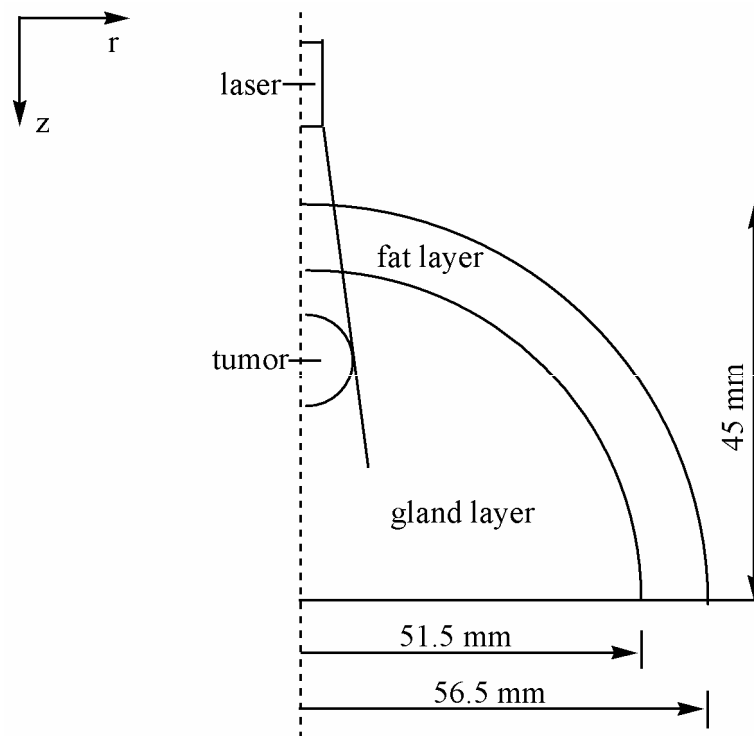


Figure 2 Breast model schematic adopted from He et al. [1]

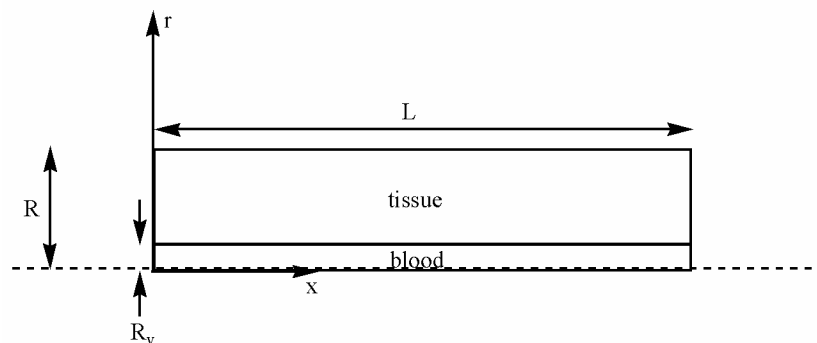


Figure 3 Capillary / tumor tissue model schematic adopted from He et al. [1]

Design Objectives

The overall goals of our study were to

1. Simulate heat transfer due to laser irradiation of the tumor; that is, model the temperature distribution in the tumor and surrounding breast tissue
2. Model blood flow through a capillary and the effect of changing temperature on the dialation/constriction of the vessel and consequently on the flow rates
3. Examine the effect of laser irradiation on blood oxygen levels in the tumor
4. Study the effects of varying exposure time, laser intensity, cooling methods, and blood and tissue properties

These goals were achieved via two finite element models using the geometries shown above and the data flow scheme depicted in Figure 4.

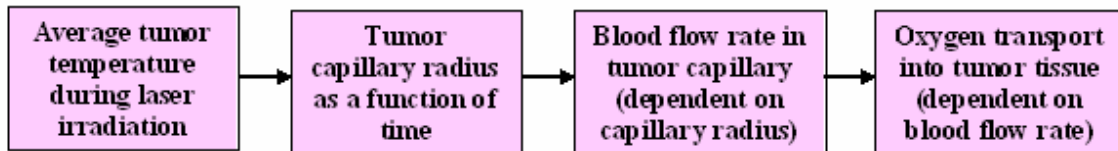


Figure 4 Flow chart describing data transfer between the breast and capillary models used in our study.

Results and Discussion

Simulation Results

Transient analysis of temperature in the breast during laser treatment gave a temperature surface plot after 900s of heating (Fig. 5a) that is qualitatively very similar to that reported by He et al [1].

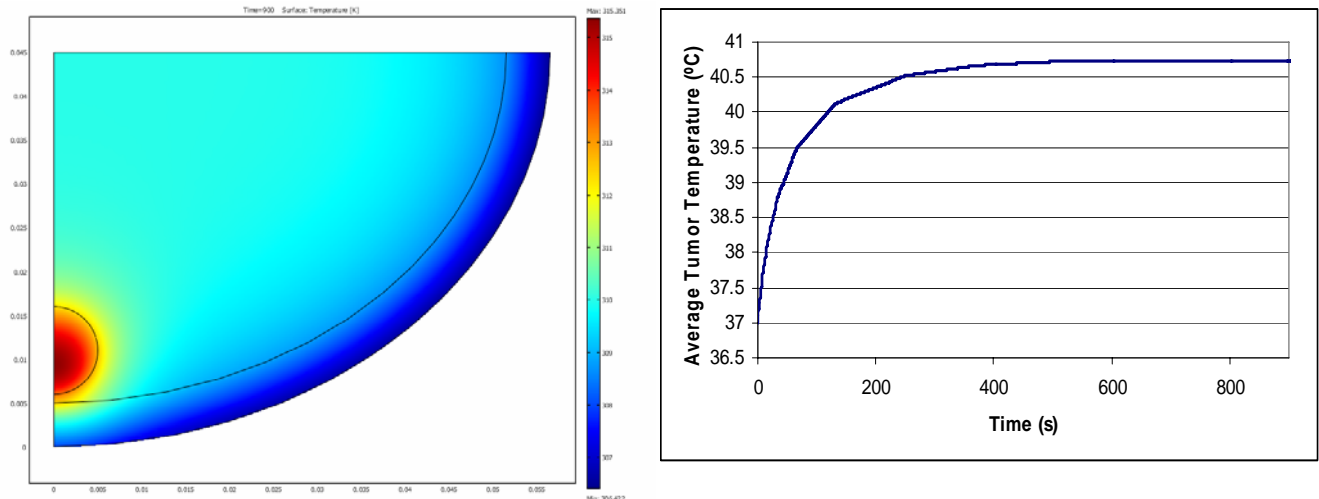


Figure 5 a) Temperature surface plot of breast following 900s of laser heating. b) Average tumor temperature over time during laser heating.

As can be seen in the temperature profile, significantly elevated temperatures are limited to the tumor and only a small portion (~1-2 mm) of surrounding healthy tissue. Moreover, the relationship between average tumor temperature and time was also very similar to that observed by He et al [1]. Using this average tumor temperature data, tumor capillary radius as a function of time was obtained with the coupling equation used by He et al [1].

After initializing the tumor blood flow simulation with steady-state solutions of the flow and diffusion governing equations, transient flow and diffusion analysis was performed in which the time-varying capillary radius was implemented as a moving boundary in the capillary/tissue geometry. The resulting oxygen concentration surface plot (Fig 6b) showed significantly increased tissue oxygen concentration relative to the steady-state solution (Fig 6a). This result follows intuition, since increasing capillary radius while maintaining a constant pressure drop across the capillary increases volumetric blood flow through the capillary and thus total oxygen flux into the capillary, which leads to increased oxygen delivered to the tissue.

By plotting partial pressure of oxygen as a function of radius r at three different points in the tissue (Fig 7), we observed that the oxygen concentration was greatest near the inlet and lowest near the outlet (as expected), and that at all three sections of the tissue, heating increased the tissue oxygen concentration to about the same extent. These plots were again found to be in close agreement with data reported by He et al. [1], confirming the validity of our model.

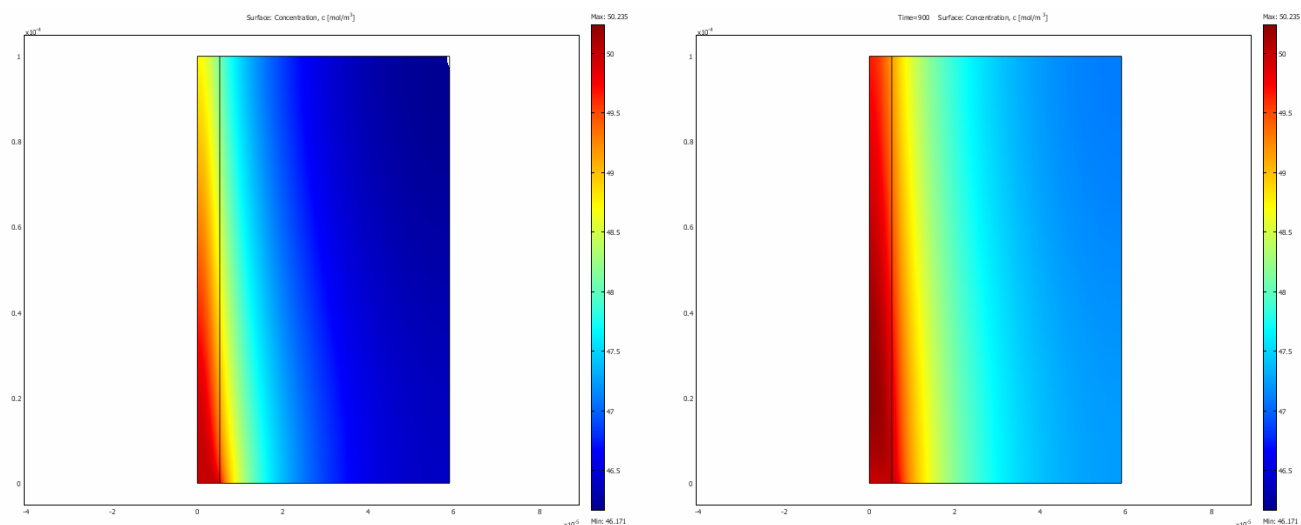


Figure 6 Oxygen concentration surface plot in the tumor capillary and tissue a) at steady state and b) following 900s of laser heating.

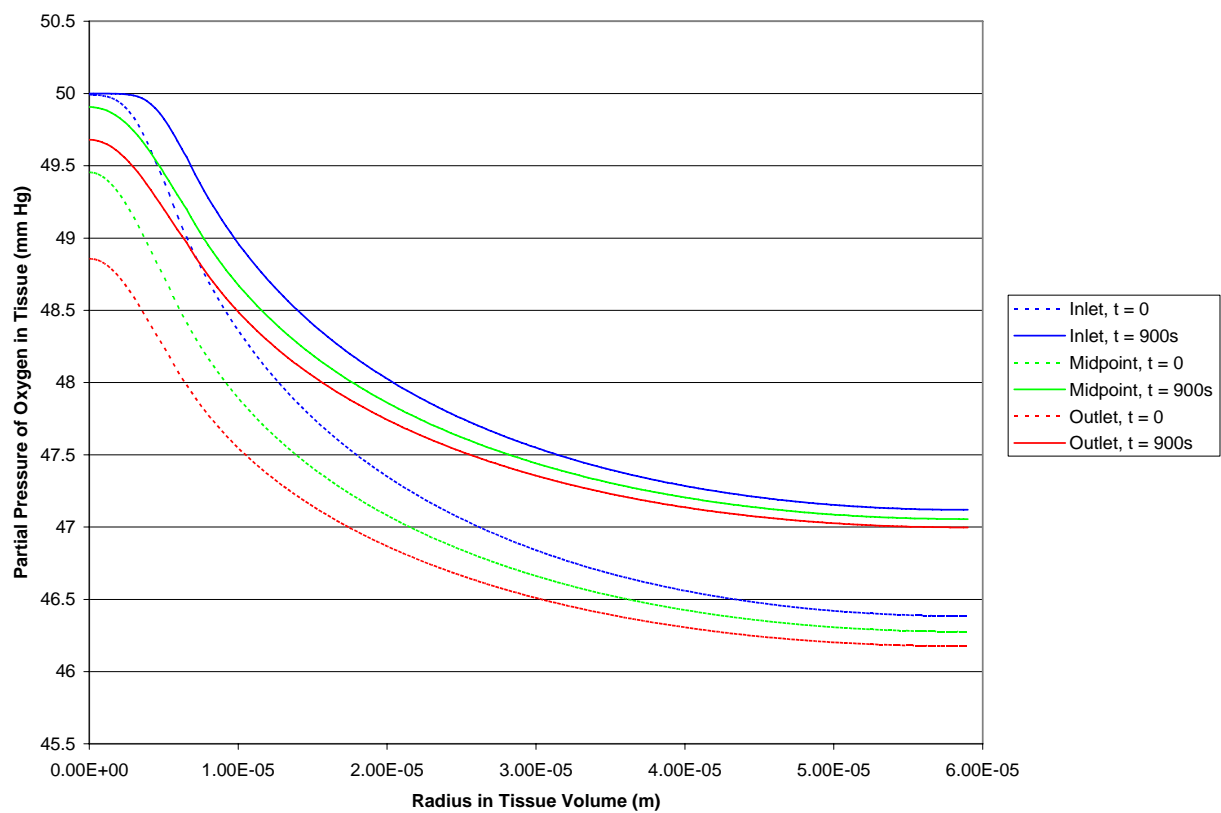


Figure 7 Partial pressure of oxygen as a function of radius in tissue at a) “inlet”: $x = 0.01$ mm b) “midpoint”: $x = 0.05$ mm c) “outlet”: $x = 0.09$ mm.

Sensitivity Analysis

I. Cooling at the Breast Surface

In order to investigate the importance of the boundary conditions at the breast surface, we examined two scenarios: a cooling flow of 10°C water over the breast surface with $h = 458 \text{ W/m}^2\text{k}$ (as used by He et al. [1]) and room temperature (25°C) air at the breast surface with $h = 13.5 \text{ W/m}^2\text{k}$ (as used by Ng et al. [5]). Our results showed that the former condition resulted in an overall cooling of the breast and tumor over time, due to the dominating effect of the cooling water, as opposed to the desirable temperature-time plot observed for the air boundary condition (Figure 8).

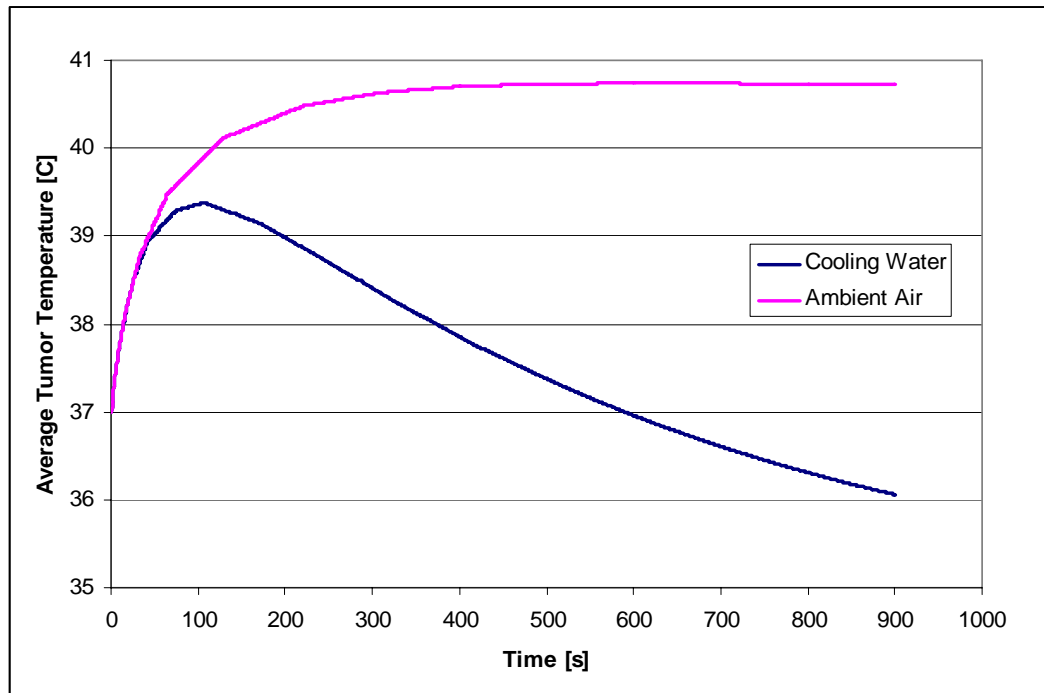


Figure 8 Average tumor temperature versus time for cooling water and ambient air boundary conditions at the breast surface.

Hence, for this reason and because it more closely matches reality (that is, it would be unrealistic to maintain a flow of water with such high convective heat transfer coefficient over the breast surface during laser treatment), we chose to use the air boundary condition throughout our study.

II. Heating Time

We tested heating times of 0, 150, 300, 600, and 900 seconds and plotted the partial pressure of oxygen as a function of radius r at $x = 0.05 \text{ mm}$ (tissue midpoint). From the plots (Fig 9), we saw that laser heating increased tissue oxygen concentration significantly (relative to before heating, shown as the blue dashed line) after only 150s, and after 600s of treatment, the oxygen concentration profile in the tissue reached a near-steady state.

Hence, tissue oxygen concentration was found to be very sensitive to heating time initially, and then virtually insensitive to it after a certain threshold (~600s).

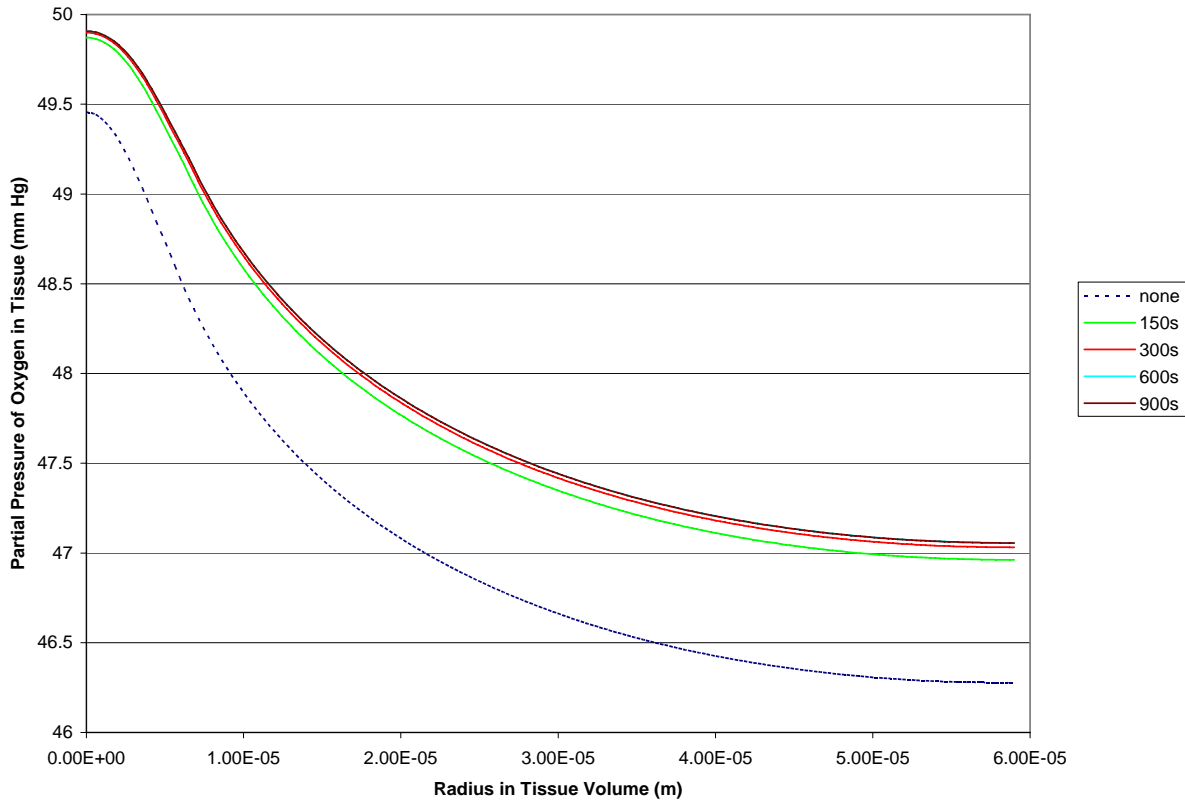


Figure 9 Oxygen concentration profile at tissue midpoint following heating for various heating periods.

III. Diffusivity of Oxygen in Blood and Tissue

In order to investigate the sensitivity of our model to diffusivity values for oxygen in blood and tissue, we varied the literature values ($1.86 \times 10^{-9} \text{ m}^2/\text{s}$ and $1.50 \times 10^{-9} \text{ m}^2/\text{s}$ for blood [7] and tissue [1], respectively) by $\pm 20\%$ and observed the resulting oxygen concentration profiles at the tissue midpoint (Fig 10-11). We observed that varying the diffusivity of oxygen in blood had a very minor effect on our results: varying the parameter by $\pm 20\%$ resulted in only about $\pm 0.1\%$ difference in the average P_{O_2} at the tissue midline after 900s of heating. Hence, our model showed little sensitivity to the diffusivity of oxygen in blood. However, varying the diffusivity of oxygen in tissue by $\pm 20\%$ resulted in about $\pm 1\%$ difference in the average P_{O_2} at the tissue midline after 900s of heating. Hence, our model was found to be about one order of magnitude more sensitive to the diffusivity of oxygen in tissue than the diffusivity of oxygen in blood. This result is illustrated in Figure 12, in which the much steeper slope of the tissue curve versus the blood curve is indicative of our model's greater sensitivity to oxygen diffusivity in tissue versus in blood.

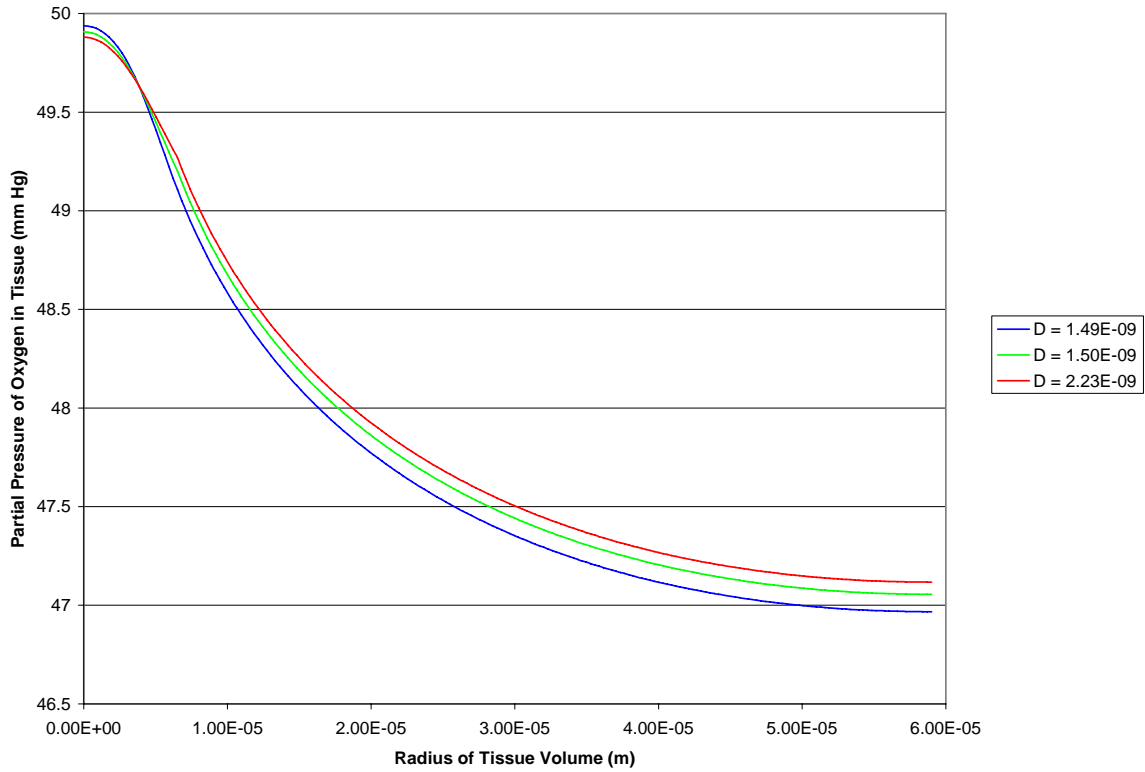


Figure 10 Oxygen concentration profiles at the tissue midpoint for varying values of diffusivity of oxygen in blood.

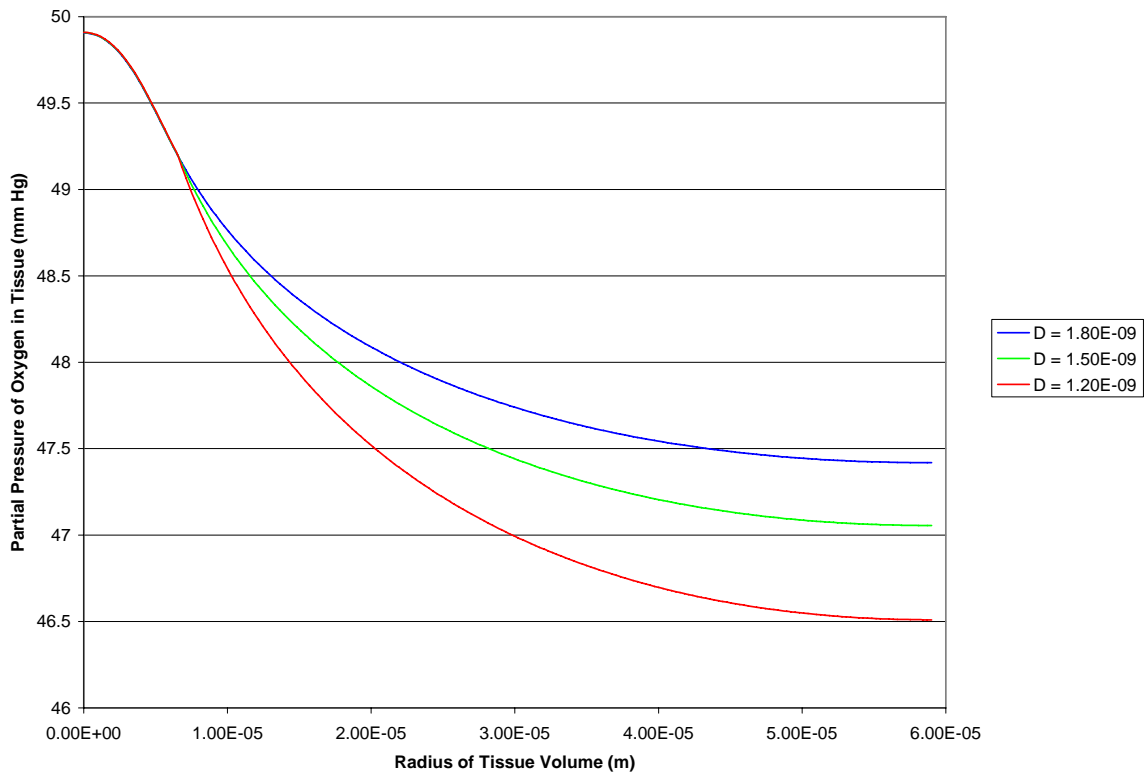


Figure 11 Oxygen concentration profiles at the tissue midpoint for varying values of diffusivity of oxygen in tissue.

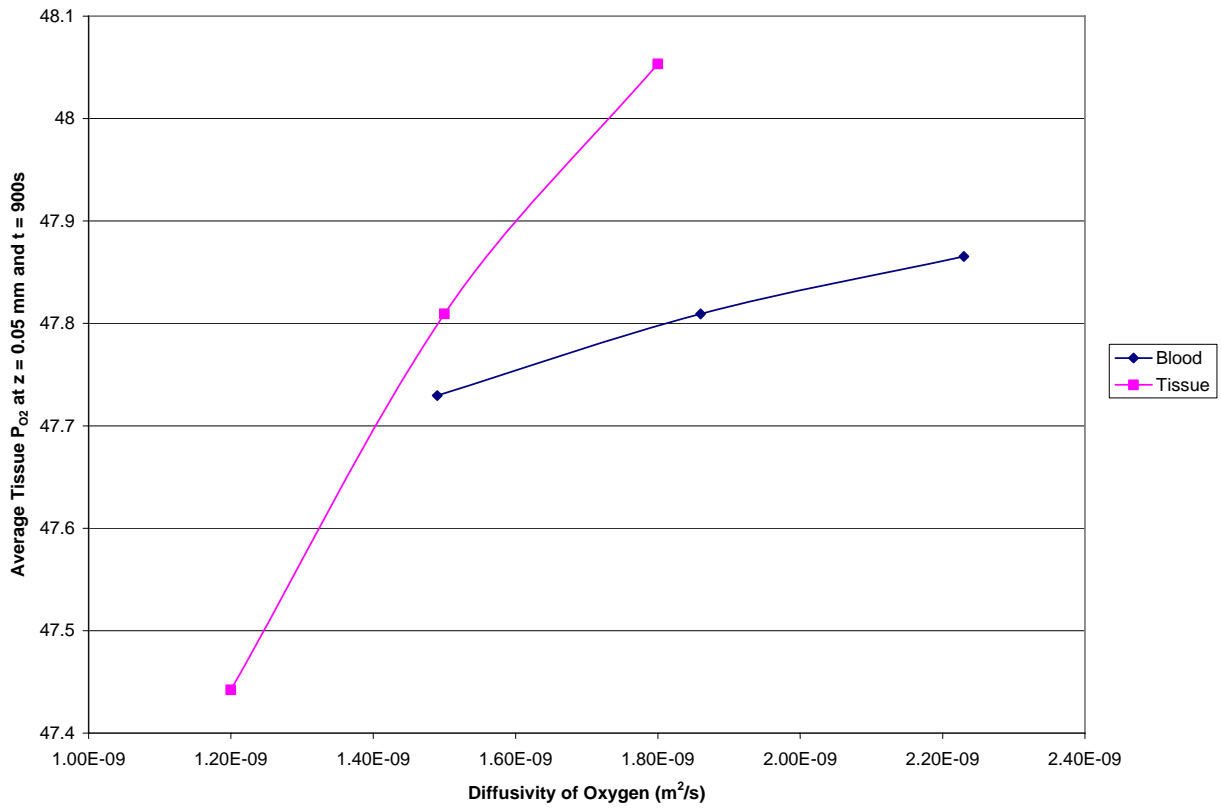


Figure 12 Effect of oxygen diffusivity value in blood and tissue on average tissue P_{O_2} at the tissue midline after 900s of heating.

IV. Laser Intensity

In order to both examine the sensitivity of our model to laser intensity and determine an optimal laser intensity to be used in hyperthermia treatment of breast tumors, we varied the laser intensity used (13000 W/m^2) by $\pm 20\%$ and 40% and examined the effect on average tumor temperature over time. Results are shown in Figure 13. As can be seen in the figure, increasing the laser intensity by 2500 W/m^2 ($\sim 20\%$ of the value used in most of our study, 13000 W/m^2) results in approximately a 0.7°C ($\sim 1.5\%$) increase in the near-steady state average temperature achieved in the tumor. Also of note is that the temperature-time curve for $I = 13000 \text{ W/m}^2$ is the lowest that appears to level off; that is, for intensities below this value, it appears that temperature begin to gradually decline after about 650-800s. Since laser treatment of a tumor would be ideally be carried out at a sustained temperature for about an hour [8], this is an important consideration and thus it would appear that a laser intensity of 13000 W/m^2 or higher would be ideal. Moreover, the literature shows that a target temperature of around $42\text{-}43^\circ\text{C}$ is suitable for treatment [8]. According to this, our model results suggest that a laser intensity of 18000 W/m^2 would be optimal.

In order to gauge the effect of treatment with laser intensity of 18000 W/m^2 on tissue oxygen concentration, we ran the moving mesh blood flow model for a simulation time of 900s

using blood vessel radius values determined from the $I = 18000 \text{ W/m}^2$ curve above. Results are shown in Figure 14.

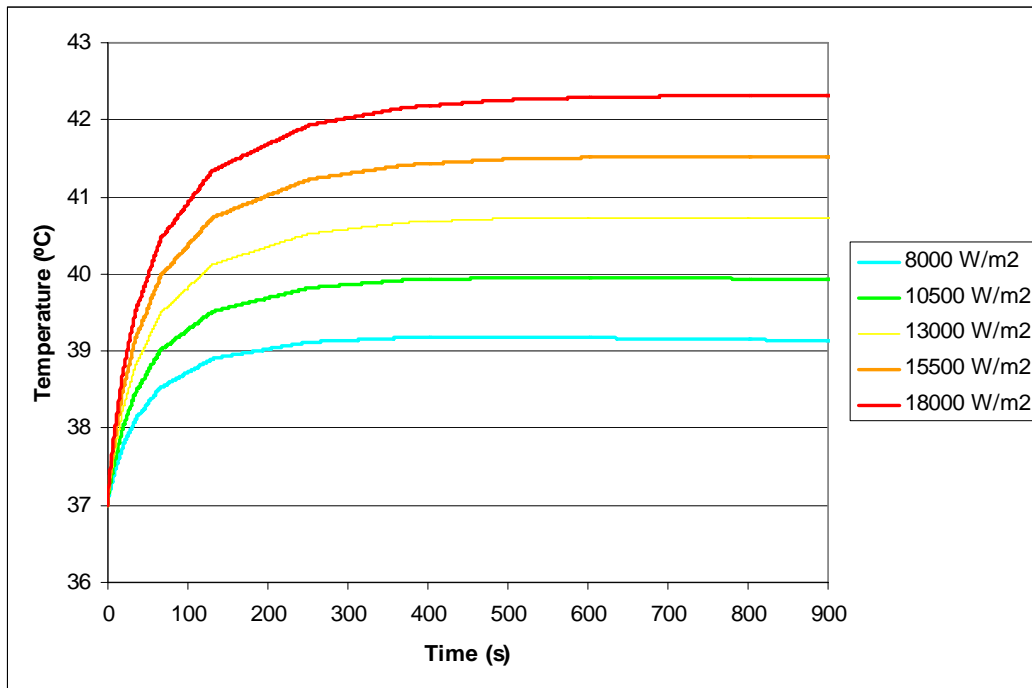


Figure 13 Average tumor temperature over time during irradiation with laser of various intensities.

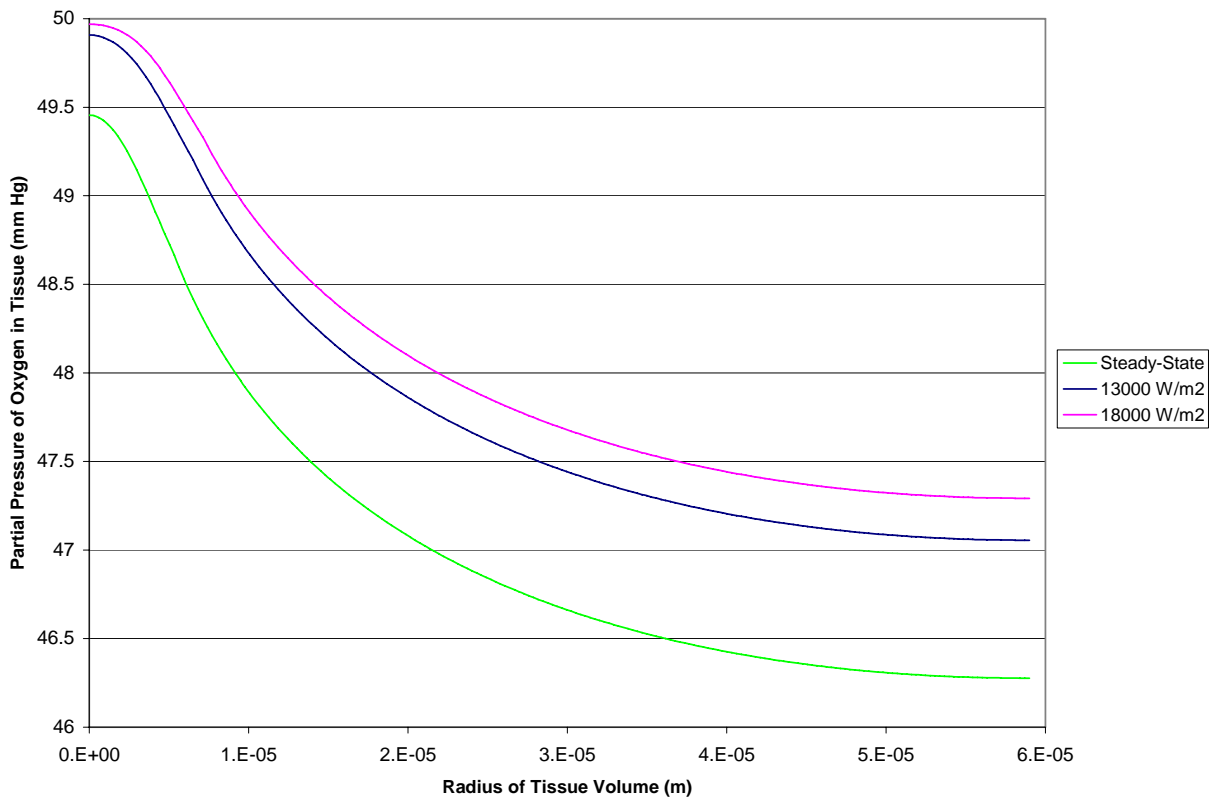


Figure 14 Oxygen concentration profiles at the tissue midpoint before laser treatment (steady-state) and for 900s of laser irradiation at 13000 W/m^2 and 18000 W/m^2 .

Relative to treatment with laser at 13000 W/m^2 , only about 0.5% difference in average tissue partial pressure of oxygen was observed when a laser intensity of 18000 W/m^2 was used. Hence, our model is only moderately sensitive to laser intensity at the tissue oxygen concentration level, as a 40% increase in laser intensity brought about only a 0.5% increase in average tissue oxygen levels. It can also be seen that relative to steady-state conditions, treatment with 18000 W/m^2 laser for 900s resulted in $\sim 1 \text{ mm Hg}$ difference in tissue oxygen partial pressure far from the capillary. Since this is the difference in tissue oxygen levels associated with raising the average tumor temperature from 37°C to about 42.5°C (as has been shown to be effective for hyperthermia treatment [8]), it can be concluded that, according to our model, a difference in tissue oxygen partial pressure of only about 1 mm Hg may be significant.

Conclusions and Design Recommendations

We have developed finite element models of a female breast with tumor and a plug of tumor tissue with a capillary whose radius varies with temperature in order to study the effects of laser irradiation on tissue oxygen levels in the tumor. Our model, which was validated primarily by comparison to a very similar—albeit more complex—model, clearly shows that laser irradiation of a breast tumor for over 600s can increase the partial pressure of oxygen in the tissue by 0.75 – 1 mm Hg. That is, with no treatment the P_{O_2} level is 0.75 – 1 mm Hg lower than in the case of any amount of laser irradiation. While such a slight change may seem insignificant, the impact of such a change is difficult to quantify without experimentation because of the complexity of coupling radiation therapy with our current model. Indeed, in the literature there does not seem to be any specific percent decrease in tissue oxygen levels that corresponds to increased radiosensitivity. However, experimental evidence shows that laser treatment for an hour at around 42.5°C is ideal for hyperthermia treatment [8].

Based on our sensitivity analysis, we recommend that a laser intensity of 18000 W/m² be employed for hyperthermia treatment of breast tumors for the purpose of increasing tumor cell radiosensitivity. This intensity was deemed ideal for two reasons: (1) it resulted in a near-steady-state average tumor temperature after a brief initial period of about 600s and (2) it increase the average tumor temperature to about 42.5°C, which is squarely in the range of ideal temperature for hyperthermia treatment [8]. Moreover, we recommend that a cooling air boundary condition be used. Our model suggests that flowing 10°C water over the surface of the breast results in a net cooling (rather than heating) of the tumor, which clearly is undesirable. In contrast, an ambient air boundary condition at the breast surface gave an ideal curve for the average tumor temperature over time—that is, one in which a constant temperature is reached quickly and sustained over time. Again, while we were unable to use a target tissue oxygen level for treatment optimization purposes, we contend that the model we have developed may be useful for this purpose once adequate experimental data is available. In addition, a model of radiation therapy could be added to it in order to directly predict the effect of laser irradiation on radiosensitivity of tumor cells.

Hyperthermia treatment is attractive because it increases the sensitivity of tumor cells to radiation treatment and thus increases its efficacy. In doing so, it improves this widely-used non-invasive treatment for malignant tumors. The main alternative to radiation therapy is tumor excision surgery, which is highly invasive and thus poses a significant health risk (as does any surgical procedure). Hence, radiation therapy allows patients to avoid the dangers of surgery, and hyperthermia treatment helps to eliminate some of the danger of radiation therapy by potentially reducing the amount of radiation employed in each treatment and the number or frequency of treatments. In a similar manner, hyperthermia treatment can reduce costs to both health care providers and patients by avoiding operations and reducing the number of radiation treatments. Thus, laser-induced hyperthermia coupled with radiation therapy has significant health and safety as well as economic implications for patients afflicted with breast tumors and health care providers tasked with treating them.

Appendix A: Mathematical Model

Geometry

Our problem is divided into two separate but linked models of different geometries. This is done in order to accommodate viewing the problem on a macro and micro scale of the breast tissue and tumor. Our analysis first looks at the breast in whole as the tumor is subjected to laser irradiation. Once the average tumor temperature as a function of time is obtained, that data is implemented into the micro scale model of the tumor. This model examines the oxygen concentration as it flows through the blood and diffuses throughout the tumor tissue. The two models are linked by a coupling equation. This equation relates the average tumor temperature to the radius of the capillary in the tumor tissue. Physiologically, as the temperature of the tumor increases the blood vessels within the tissue dilate in order to cool the tissue.

Governing Equations

Breast Model

$$\rho c \frac{\partial T}{\partial t} = k \left(\frac{\partial^2 T}{\partial r^2} + \frac{1}{r} \frac{\partial T}{\partial r} + \frac{\partial^2 T}{\partial z^2} \right) + Q + \omega \rho_b c_b (T_b - T) \quad (\text{Heat Transfer})$$

$$\text{where } Q = a I_0 e^{-az}$$

Capillary / Tumor Tissue Model

$$\alpha \frac{\partial P_{O_2}}{\partial t} = D \alpha \left(\frac{\partial^2 P_{O_2}}{\partial r^2} + \frac{\partial^2 P_{O_2}}{\partial z^2} \right) - u \alpha \frac{\partial P_{O_2}}{\partial r} + R \quad (\text{Mass Transfer})$$

$$\rho \left(\frac{\partial u}{\partial t} + u \cdot \nabla u \right) = -\nabla p + \mu \nabla^2 u + \rho g \quad (\text{Fluid Flow})$$

Coupling Equation

$$r = r_0 \sqrt{e^{b(T-T_0)}}, \quad \text{where } b = \begin{cases} 0.1 & T = 39 - 42^\circ \text{C} \\ -0.1 & T > 42^\circ \text{C} \end{cases}$$

Initial Conditions

Breast Model

- The entire breast is initially at body temperature 37°C (310 K).

Capillary / Tumor Tissue Model

Fluid Flow

- The velocities in the R- and Z-directions were found by first solving the steady-state problem. Then the solutions for the velocities were used as the initial conditions for the transient analysis.

Diffusion

- The concentrations in the blood and the tissue were found by first solving the steady-state problem. Then the solutions for the concentrations were used as the initial conditions for the transient analysis.

Boundary Conditions

Breast Model

- Along Z-axis: axial symmetry
- Along R-axis (at $z = 0.45$ mm): thermal insulation, zero heat flux
- Along Breast Surface: heat flux = $h(T_{surface} - T_{\infty})$

Capillary / Tumor Tissue Model

Fluid Flow

- $z = 0, r \leq R_v: p = 2306$ Pa
- $z = L, r \leq R_v: p = 1160$ Pa
- $r = R_v$: no slip
- $r = 0$: axial symmetry
- $z = 0, r \leq R_v: p = 2306$ Pa

Diffusion

- $z = 0, r \leq R_v: P_{O_2} = 50$ mm Hg
- $z = 0, R_v \leq r \leq R$ or $z = L, R_v \leq r \leq R$: zero flux, $\frac{\partial P_{O_2}}{\partial z} = 0$
- $r = 0$ or $r = R$: $\frac{\partial P_{O_2}}{\partial r} = 0$

Input Parameters

Breast Model

Dimensions (taken from He et al. [1])

- see schematic (page 4)

Properties

Table A1 Laser properties (taken from He et al. [1])

Intensity	W/m^2	13000
Alpha	m^{-1}	100

Table A2 Blood perfusion properties (taken from Ng et al. [5])

	$c_b W_b$
Layer	$(W/m^3 * ^\circ C)$
Fat	800
Gland	2400
Tumor	48000

Table A3 Boundary properties (taken from He et al. [1] and Ng et al. [5])

Cooling Method		10°C Water	Ambient Air
Heat Transfer Coefficient (h)	$W/m^2 * K$	458 [1]	13.5 [5]
External Temperature (T_{inf})	K	283	298

Table A4 Subdomain properties (taken from He et al. [1])

		Fat	Tissue	Tumor	Blood
Density	$kg * m^{-3}$	930	1050	1050	1100
Specific Heat	$J * kg^{-1} * K^{-1}$	2770	3770	3770	3300
Thermal Conductivity	$W * m^{-1} * K^{-1}$	0.22	0.48	0.48	0.45

Capillary / Tumor Tissue Model

Dimensions (taken from He et al. [1])

$$R_v = 6 \mu m$$

$$R = 60 \mu m$$

$$L = 100 \mu m$$

Fluid Flow Properties

Table A5 Boundary properties (taken from Jain [6])

		Inlet	Outlet
Pressure	mm Hg	2306	1160

Table A6 Subdomain properties (taken from He et al. [1] and Yoshida et al. [7])

		Blood
Density	kg/m ³	1100 [1]
Dynamic Viscosity	Pa*s	0.0044 [1]
Diffusion Coefficient	m ² /s	1.86E-09 [7]

Diffusion Properties

Table A7 Boundary properties (taken from He et al. [1])

		Inlet
Oxygen Partial Pressure	mm Hg	50

Table A8 Subdomain properties (taken from He et al. [1] and Yoshida et al. [7])

		Blood	Tumor
Diffusion Coefficient	m ² /s	1.86E-09 [7]	1.50E-09 [1]
Reaction Rate	mol/m ³ *s	NA	-1.1 [1]

Appendix B: Mesh

Breast Model

The breast model mesh was divided into three regions: tissue layer, subcutaneous fat layer, and tumor layer (see Appendix A for dimensions). For this model, triangular elements were employed with a slight increase in mesh density in and around the tumor region. The total number of elements used was 2089.

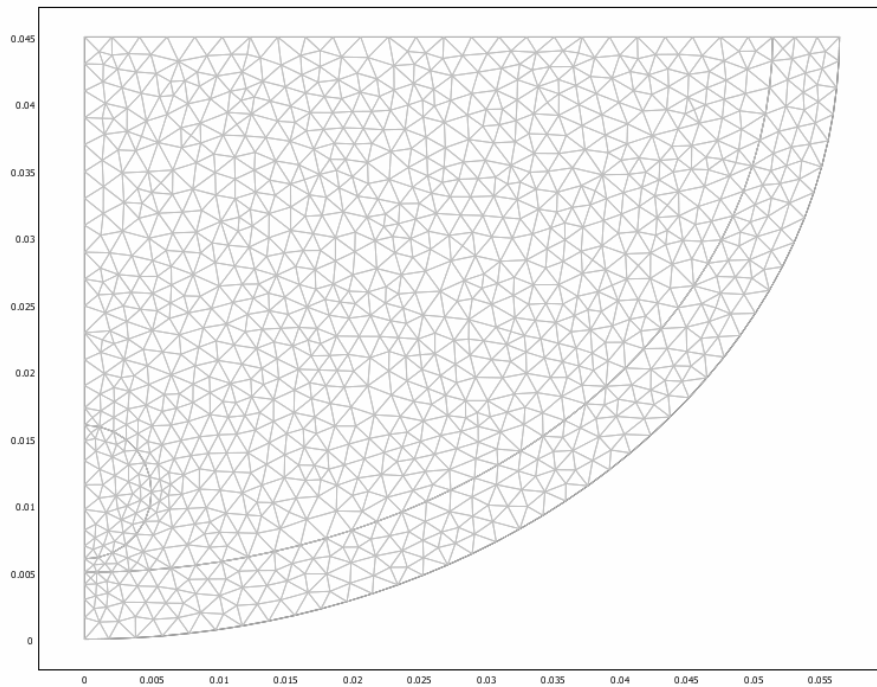


Figure B1 Breast model mesh

Capillary / Tumor Tissue Model

The breast model mesh was divided into two regions: the capillary and the tumor tissue (see Appendix A for dimensions). For this model, quadrilateral elements were mapped with an increasing mesh density near the blood vessel, the region of highest flux. The total number of elements used was 3000.

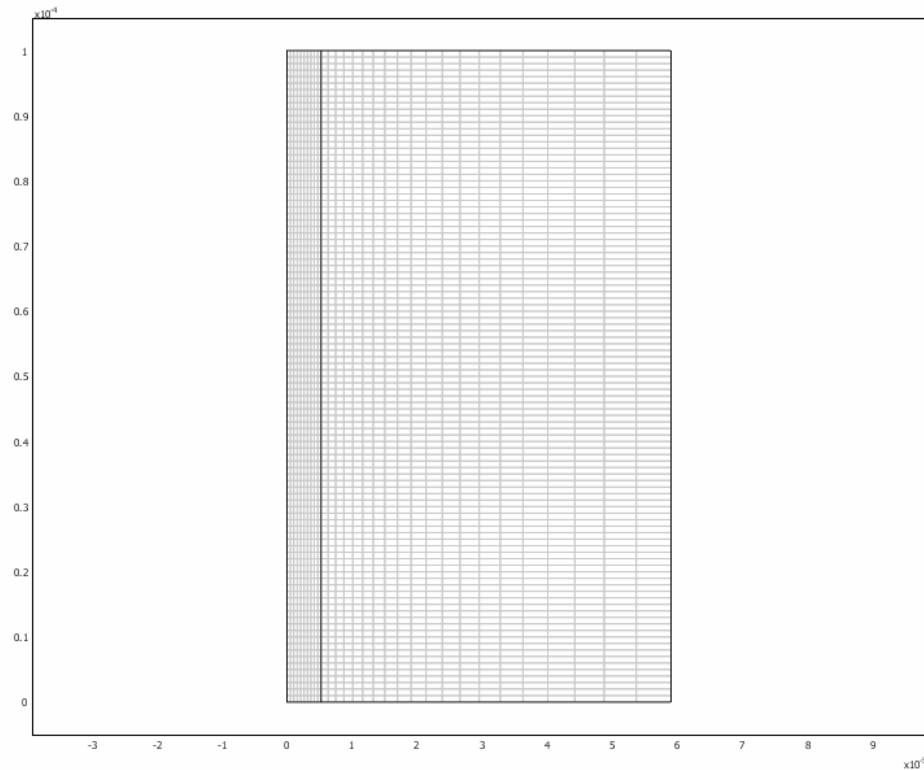


Figure B2 Capillary / tumor tissue mesh

Mesh Convergence

For each of the two geometries used in our problem, we performed mesh convergence analysis. Each geometry was meshed with a progressively higher number of elements and the value of average tumor temperature after 900s (breast model) and average partial pressure of oxygen along the tissue midline after 900s (blood flow model) was measured. Results obtained are summarized in Fig. B3-B4.

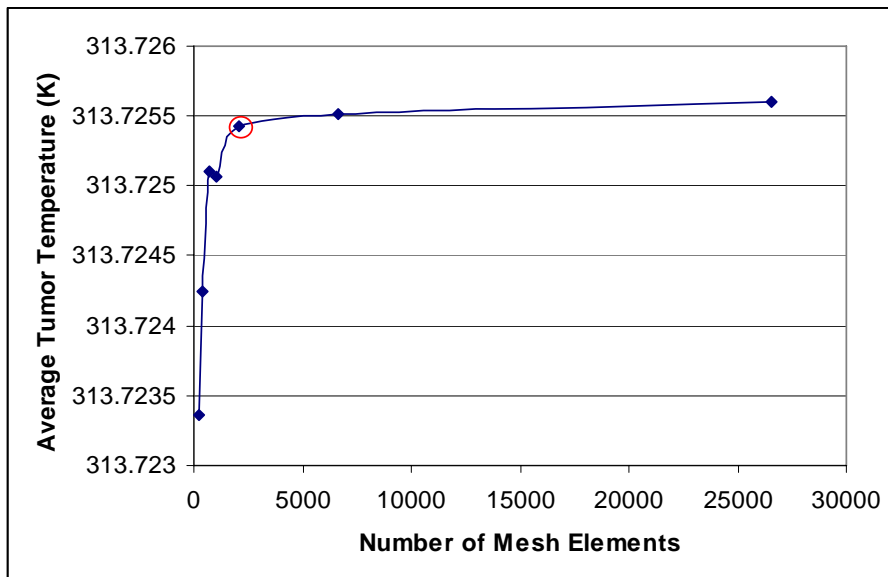


Figure B3 Mesh convergence for the breast model. Red circle denotes the actual number of mesh elements used in the simulation.

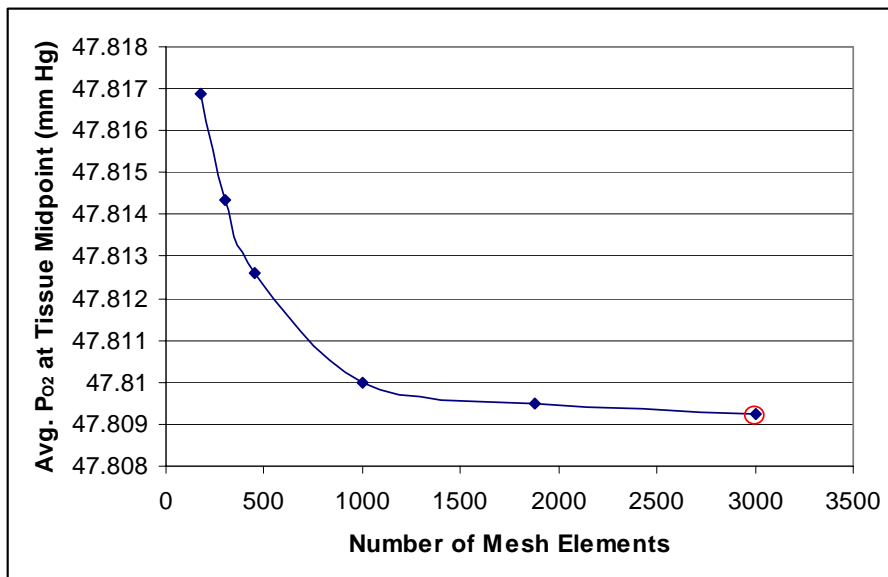


Figure B4 Mesh convergence for the capillary blood flow model. Red circle denotes the actual number of mesh elements used in the simulation.

As can be seen, mesh convergence was obtained for both geometries, and an appropriate number of mesh elements was chosen for each case such that the solution was independent of the number of mesh elements used.

Appendix C: References

1. He Y, Shirazaki M, Lui H, Himeno R, Sun Z. A numerical coupling model to analyze the blood flow, temperature, and oxygen transport in human breast and tumor under laser irradiation. *Computers in Biology and Medicine*. 36 (2006): 1336-1350.
2. All About Breast Cancer. *American Cancer Society*. Accessed 24 April 2007. <http://www.cancer.org/docroot/CRI/CRI_2x.asp?sitearea=&dt=5>.
3. Song CW, Park H, Griffin RJ. Improvement of Tumor Oxygenation by Mild Hyperthermia. *Radiation Research*. 55(4) (2001): 515-528.
4. Itani W, Geara F, Haykal J, Haddadin M, Gali-Muhtasib H. Radiosensitization by 2-benzoyl-3-phenyl-6,7-dichloroquinoxaline 1,4-dioxide under oxia and hypoxia in human colon cancer cells. *Radiation Oncology*. 2(1) (2007).
5. Ng EYK and Sudharsan NM. An improved three-dimensional direct numerical modeling and thermal analysis of a female breast with tumor. *Proceedings Institution of Mechanical Engineers*. 215 (2001).
6. Jain RK. Determinants of Tumor Blood Flow: A Review. *Cancer Research*. 48 (1988): 2641-2658.
7. Yoshida F and Ohshima N. Diffusivity of oxygen in blood serum. *Journal of Applied Physiology*. 21(3) (1966): 915-919.
8. Zhu D, Lu W, Weng Y, Cui H, Luo Q. Monitoring thermal-induced changes in tumor blood flow and microvessels with laser speckle contrast imaging. *Applied Optics*. 46(10) (2007): 1911-1917.